Integrated holographic system for all-optical manipulation of developing embryos

Maria Leilani Torres-Mapa,[1,*] Maciej Antkowiak,[2,3] Hana Cizmarova,[1] David E. K. Ferrier,[3,4] Kishan Dholakia,[1,5] and Frank J. Gunn-Moore[2,5]

[1]*SUPA, School of Physics and Astronomy, University of St. Andrews, Fife, KY169SS, UK*
[2]*SULSA,University of St. Andrews, Fife, KY169SS, UK*
[3]*School of Biology, University of St. Andrews, Fife, KY169SS, UK*
[4]*The Scottish Oceans Institute, University of St. Andrews, Fife KY168LB, UK*
[5]*Contributed equally to this work*
**mlt9@st-andrews.ac.uk*

Abstract: We demonstrate a system for the combined optical injection and trapping of developing embryos. A Ti:sapphire femtosecond laser in tandem with a spatial light modulator, is used to perform fast and accurate beam-steering and multiplexing. We show successful intracellular delivery of a range of impermeable molecules into individual blastomeres of the annelid *Pomatoceros lamarckii* embryo by optoinjection, even when the embryo is still enclosed in a chorion. We also demonstrate the ability of the femtosecond laser optoinjection to deliver materials into inner layers of cells in a well-developed embryo. By switching to the continuous wave mode of the Ti:sapphire laser, the same system can be employed to optically trap and orient the 60 μm sized *P. lamarckii* embryo whilst maintaining its viability. Hence, a complete all-optical manipulation platform is demonstrated paving the way towards single-cell genetic modification and cell lineage mapping in emerging developmental biology model species.

OCIS codes: (170.1420) Biology; (020.4180) Multiphoton processes; (140.3538) Lasers, pulsed; (140.7090) Ultrafast lasers; (350.4855) Optical tweezers or optical manipulation

References and links

1. G. Thalhammer, R. Steiger, S. Bernet, and M. Ritsch-Marte, "Optical macro-tweezers: trapping of highly motile micro-organisms," J. Opt. **13**(4), 044024 (2011).
2. D. J. Stevenson, F. Gunn-Moore, and K. Dholakia, "Light forces the pace: optical manipulation for biophotonics," J. Biomed. Opt. **15**(4), 041503 (2010).
3. D. J. Stevenson, F. J. Gunn-Moore, P. Campbell, and K. Dholakia, "Single cell optical transfection," J. R. Soc. Interface **7**(47), 863–871 (2010).
4. P. Mthunzi, K. Dholakia, and F. Gunn-Moore, "Phototransfection of mammalian cells using femtosecond laser pulses: optimization and applicability to stem cell differentiation," J. Biomed. Opt. **15**(4), 041507 (2010).
5. D. L. Wokosin, J. M. Squirrell, K. W. Eliceiri, and J. G. White, "Optical workstation with concurrent, independent multiphoton imaging and experimental laser microbeam capabilities," Rev. Sci. Instrum. **74**(1), 193–201 (2003).
6. C. T. A. Brown, D. J. Stevenson, X. Tsampoula, C. McDougall, A. A. Lagatsky, W. Sibbett, F. J. Gunn-Moore, and K. Dholakia, "Enhanced operation of femtosecond lasers and applications in cell transfection," J Biophotonics **1**(3), 183–199 (2008).
7. C. Xie, M. A. Dinno, and Y. Q. Li, "Near-infrared Raman spectroscopy of single optically trapped biological cells," Opt. Lett. **27**(4), 249–251 (2002).
8. J. Guck, R. Ananthakrishnan, H. Mahmood, T. J. Moon, C. C. Cunningham, and J. Käs, "The optical stretcher: a novel laser tool to micromanipulate cells," Biophys. J. **81**(2), 767–784 (2001).
9. I. M. Tolić-Nørrelykke, E.-L. Munteanu, G. Thon, L. Oddershede, and K. Berg-Sørensen, "Anomalous diffusion in living yeast cells," Phys. Rev. Lett. **93**(7), 078102 (2004).
10. H. Liang, K. T. Vu, P. Krishnan, T. C. Trang, D. Shin, S. Kimel, and M. W. Berns, "Wavelength dependence of cell cloning efficiency after optical trapping," Biophys. J. **70**(3), 1529–1533 (1996).
11. Y. Liu, D. K. Cheng, G. J. Sonek, M. W. Berns, C. F. Chapman, and B. J. Tromberg, "Evidence for localized cell heating induced by infrared optical tweezers," Biophys. J. **68**(5), 2137–2144 (1995).

#141509 - $15.00 USD Received 21 Jan 2011; revised 17 Apr 2011; accepted 13 May 2011; pub. 16 May 2011

12. G. M. Akselrod, W. Timp, U. Mirsaidov, Q. Zhao, C. Li, R. Timp, K. Timp, P. Matsudaira, and G. Timp, "Laser-guided assembly of heterotypic three-dimensional living cell microarrays," Biophys. J. **91**(9), 3465–3473 (2006).
13. K. C. Neuman, E. H. Chadd, G. F. Liou, K. Bergman, and S. M. Block, "Characterization of photodamage to *Escherichia coli* in optical traps," Biophys. J. **77**(5), 2856–2863 (1999).
14. W. Choi, S.-W. Nam, H. Hwang, S. Park, and J.-K. Park, "Programmable manipulation of motile cells in optoelectronic tweezers using a grayscale image," Appl. Phys. Lett. **93**(14), 143901 (2008).
15. J. K. Valley, P. Swinton, W. J. Boscardin, T. F. Lue, P. F. Rinaudo, M. C. Wu, and M. M. Garcia, "Preimplantation mouse embryo selection guided by light-induced dielectrophoresis," PLoS ONE **5**(4), e10160 (2010).
16. A. Vogel, J. Noack, G. Huttman, and G. Paltauf, "Mechanisms of femtosecond laser nanosurgery of cells and tissues," Appl. Phys. B **81**(8), 1015–1047 (2005).
17. V. Kohli, V. Robles, M. L. Cancela, J. P. Acker, A. J. Waskiewicz, and A. Y. Elezzabi, "An alternative method for delivering exogenous material into developing zebrafish embryos," Biotechnol. Bioeng. **98**(6), 1230–1241 (2007).
18. E. Cotter, R. O'Riordan, and A. Myers, "A histological study of reproduction in the serpulids *Pomatoceros triqueter* and *Pomatoceros lamarckii* (Annelida: Polychaeta)," Mar. Biol. **142**, 905–914 (2003).
19. D. R. Dixon, J. T. Wilson, P. L. Pascoe, and J. M. Parry, "Anaphase aberrations in the embryos of the marine tubeworm *Pomatoceros lamarckii* (Polychaeta: Serpulidae): a new in vivo test assay for detecting aneugens and clastogens in the marine environment," Mutagenesis **14**(4), 375–383 (1999).
20. C. McDougall, W. C. Chen, S. M. Shimeld, and D. E. K. Ferrier, "The development of the larval nervous system, musculature and ciliary bands of *Pomatoceros lamarckii* (Annelida): heterochrony in polychaetes," Front. Zool. **3**(1), 16 (2006).
21. T. Takahashi, C. McDougall, J. Troscianko, W. C. Chen, A. Jayaraman-Nagarajan, S. M. Shimeld, and D. E. K. Ferrier, "An EST screen from the annelid *Pomatoceros lamarckii* reveals patterns of gene loss and gain in animals," BMC Evol. Biol. **9**(1), 240 (2009).
22. R. C. Brusca, G. J. Brusca, and N. Haver, *Invertebrates* (Sinauer Associates, 2003).
23. K. Tessmar-Raible and D. Arendt, "Emerging systems: between vertebrates and arthropods, the Lophotrochozoa," Curr. Opin. Genet. Dev. **13**(4), 331–340 (2003).
24. M. Antkowiak, M. L. Torres-Mapa, F. Gunn-Moore, and K. Dholakia, "Application of dynamic diffractive optics for enhanced femtosecond laser based cell transfection," J Biophotonics **3**(10-11), 696–705 (2010).
25. I. A. Gwynn and P. C. Jones, "On the egg investments and fertilization reaction in *Pomatoceros triqueter L.*," Z. Zellforsch. Mikrosk. Anat. **113**(3), 388–395 (1971).
26. O. Seksek, J. Biwersi, and A. S. Verkman, "Translational diffusion of macromolecule-sized solutes in cytoplasm and nucleus," J. Cell Biol. **138**(1), 131–142 (1997).
27. G. L. Lukacs, P. Haggie, O. Seksek, D. Lechardeur, N. Freedman, and A. S. Verkman, "Size-dependent DNA mobility in cytoplasm and nucleus," J. Biol. Chem. **275**(3), 1625–1629 (2000).
28. J. Baumgart, W. Bintig, A. Ngezahayo, S. Willenbrock, H. Murua Escobar, W. Ertmer, H. Lubatschowski, and A. Heisterkamp, "Quantified femtosecond laser based opto-perforation of living GFSHR-17 and MTH53 a cells," Opt. Express **16**(5), 3021–3031 (2008).
29. A. Vogel, N. Linz, S. Freidank, and G. Paltauf, "Femtosecond-laser-induced nanocavitation in water: implications for optical breakdown threshold and cell surgery," Phys. Rev. Lett. **100**(3), 038102 (2008).
30. C. J. de Grauw, J. M. Vroom, H. T. M. van der Voort, and H. C. Gerritsen, "Imaging properties in two-photon excitation microscopy and effects of refractive-index mismatch in thick specimens," Appl. Opt. **38**(28), 5995–6003 (1999).
31. W. Supatto, D. Débarre, B. Moulia, E. Brouzés, J. L. Martin, E. Farge, and E. Beaurepaire, "In vivo modulation of morphogenetic movements in Drosophila embryos with femtosecond laser pulses," Proc. Natl. Acad. Sci. U.S.A. **102**(4), 1047–1052 (2005).

1. Introduction

Optical manipulation allows contact-free handling [1] and modification of microscopic biological samples. Using light, a microscopic species can be probed, trapped, sorted and optoinjected in order to understand its physiological properties and its response to a mechanical, chemical or environmental stimuli. Importantly, optical manipulation of biological samples is fully sterile, compatible with microscopic imaging and can be easily automated for high throughput image-based processing. Very often it also causes less stress and collateral damage when compared with traditional mechanical techniques, which provides much better long-term viability of manipulated samples. A focused laser beam can exert sufficient force to tweeze and orient a cell or a subcellular organelle [2]. Optical manipulation of biological samples such as cells, bacteria and DNA strands have been extensively employed as a tool for holding, stretching and characterizing sample properties [2]. At the

#141509 - $15.00 USD Received 21 Jan 2011; revised 17 Apr 2011; accepted 13 May 2011; pub. 16 May 2011

same time a pulsed focused laser beam of sufficient intensity can porate the membrane of a single cell leading to optical injection of molecules and genetic material [3,4].

An important advantage of optical manipulation is its easy reconfigurability, which provides much needed versatility in a multi-modal operation on a variety of samples. As an example, a multiphoton system can be utilized for both subsequent imaging and laser ablation [5]. Similarly, a single femtosecond (fs) laser system can be toggled between continuous wave (CW) and fs operation for optical trapping of cells and intracellular delivery of macromolecules [6], as we also show in this paper. Since optical manipulation systems are often built around microscopes, subsequent long-term imaging is possible without disturbing the sample on stage, maintaining the suitable physiological environment of the sample.

In this work we demonstrate an all-optical approach to manipulation of complex biological samples such as a developing embryo. Although optical trapping of single cells has been employed in many applications such as Raman spectroscopy [7], optical stretching [8] and microrheology measurements [9], there are very few studies on optically orienting and trapping of embryos which are tens of microns in size. Optical trapping of single cells has been employed in model systems such as CHO cells [10,11], fibroblasts [12] and *Escherichia coli* bacteria [13] with a maximum optically trapped size of ~20 μm. Optical trapping of larger specimens was often demonstrated using optoelectronic tweezers (OET) for orienting and trapping of motile specimens such as *Tetrahymena pyriformis* [14]. OET of mouse embryos has also been demonstrated for the purposes of embryo sorting prior implantation [15]. Recently, optical trapping of a variety of swimming motile specimens was reported using a dual focus mirror trap [1]. These results show that a non-contact automated optical method to move, orient and hold developing embryos would bring a clear advantage over the commonly used intrusive glass capillaries, which cause unnecessary stress in the sample and require manual dexterity,.

At the same time, there is a significant interest in finding alternatives to microinjection-based delivery of DNA, mRNA or siRNA into single cells of developing embryos for the purposes of their cell selective genetic modification. In recent years, optoinjection using NIR fs laser pulses has been found to be an effective tool in delivering different types of biomolecules into single cells with high post-treatment viability. Focused near-infrared (NIR) femtosecond (fs) lasers create a transient pore due to membrane interaction with a low density plasma created by multiphoton ionization [16]. Optical manipulation using an ultrafast NIR fs system is a robust technology for *in vivo* studies. The focused NIR fs pulses interaction with tissue or cells relies on nonlinear absorption; hence, the affected area is limited to the focal volume of the laser beam enabling a highly targeted and precise ablation *in vivo* without any collateral damage in the surrounding cells. To date, utilizing NIR fs pulses for optoinjection in an embryo has only been reported on a large ~1mm zebrafish [17]. However, the absorption, structure and size properties may be completely different with embryos of different species.

In this study, we use two modes of Ti:sapphire laser operation in a combined optical manipulation of small developing embryos. By toggling between CW and pulsed mode-locked operation, we demonstrate independent optical trapping of the 60 μm sized embryos of *Pomatoceros lamarckii* and optical injection of macromolecules into its individual blastomeres. *P. lamarckii* are marine organisms, abundant in intertidal and shallow sub-littoral zones. They are significant biofouling agent [18] and have been studied for ecotoxicology research, assaying larval survival and karyotype in the presence of potential pollutants [19]. *P. lamarckii* is also a member of the Lophotrochozoa clade of bilaterian animals which are relatively poorly represented in terms of our understanding of animal development [20,21]. Furthermore, this species is considered to be a promising model for understanding animal evolution [22,23]. However, at present there is no technology that has been demonstrated to allow successful and viable manipulation of the embryo of this species. Hence, developing optical methods for manipulation of these embryos would significantly improve our

#141509 - $15.00 USD Received 21 Jan 2011; revised 17 Apr 2011; accepted 13 May 2011; pub. 16 May 2011

capabilities in understanding the development of *P. lamarckii* and open the way to manipulate similarly sized embryos.

In this work we show how a holographic system based on a spatial light modulator (SLM) can be used as a highly flexible tool for stable trapping of an embryo and enhanced targeting of its individual blastomeres. By changing the light wavefront modulation encoded on the SLM, three dimensional beam steering and multiplexing can be achieved. Using this system, individual embryos can be positioned and oriented in 3-dimensions using a low numerical aperture (NA.) objective, allowing optical orientation and manipulation within a large-field of view. At the same time, as we have recently demonstrated [24], an SLM can be used to enhance viable optoinjection of single cells by more precise multiple targeting of their membrane. The versatility and ease-of-use offered by this combined system opens new avenues in flexible and dynamic manipulation of developing embryos.

2. Experimental design

The multi-modal holographic system for optical trapping and optoinjection shown in Fig. 1(A) is based on our previously reported setup [24]. For optoinjection experiments, we utilized a diode pumped (Coherent, Verdi V-5) Ti:sapphire fs laser (Coherent, MIRA900) operating at 180 fs, 80 MHz with its wavelength centered at 800 nm. The fs laser beam was expanded by a telescope system (L1 and L2) passing through an electronic shutter and was directed into an SLM (Hamamatsu PPM X8267-13) which provided fast spatial and axial control of the laser. The shutter triggered through a DAQ card controlled the exposure of the laser on the embryo varied from 10 ms to 60 ms. A telescope with lenses L1 and L2 with focal lengths (f) 50 mm and 1000 mm respectively expanded the beam to fill the active area of the SLM. A half-wave ($\lambda/2$) plate before the telescope rotated the polarization of laser to maximize the power diffracted into the first order. L3 (f = 500mm) and L4 (f = 200mm) relayed the SLM at the backaperture of the objective and ensured that the backaperture was overfilled. A slit is positioned at the intermediate image plane after the SLM to block the zero order and the

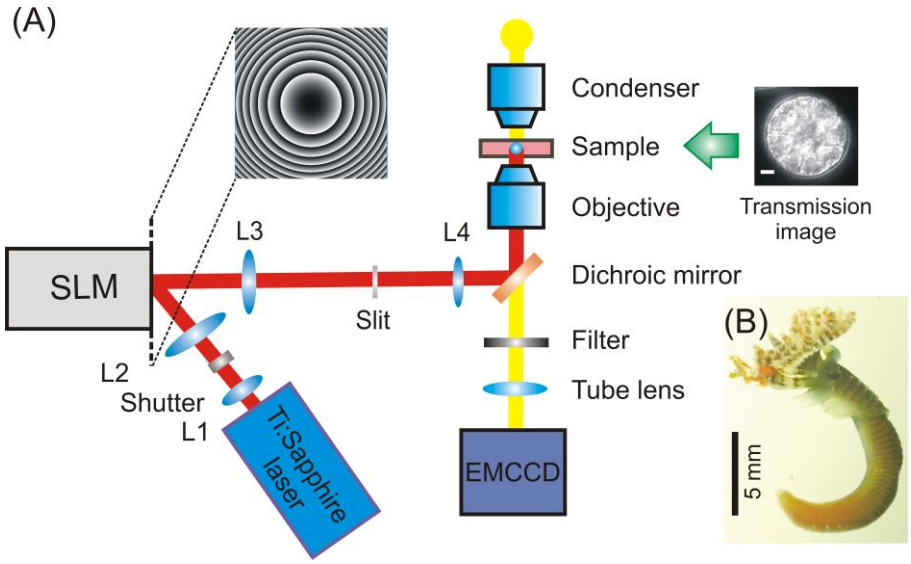

Fig. 1. (A) Schematic diagram of the integrated holographic for optical trapping and optoinjection of developing embryos. The beam was then directed to a SLM (Spatial light Modulator). A dichroic mirror deflected the fs laser to the back aperture of a 0.8 NA, x60 Nikon, microscope objective. Imaging was performed using an EMCCD camera. Bar corresponds to 10 μm. (B) Image of an adult de-tubed *P. lamarckii* worm.

#141509 - $15.00 USD Received 21 Jan 2011; revised 17 Apr 2011; accepted 13 May 2011; pub. 16 May 2011

higher-order diffraction. The laser was then directed into a Nikon TE-2000 microscope and focused into the sample by a 0.8 NA, 60x air objective (Nikon).

For optical trapping experiments, the Ti:sapphire laser was switched to CW mode operation with an output wavelength at 800 nm. The beam was directed to a 0.5 NA, 20x air objective (Nikon). The shutter was opened all throughout the experiment. The three dimensional position of the focal spot within the sample was controlled by a combination of a blazed grating and a Fresnel lens displayed on the SLM, as described before [24]. At the same time, the beam could be multiplexed by displaying a complex superposition of multiple modulations.

The system was fully equipped with Differential Interference Contrast (DIC) and epi-fluorescence imaging based on an EMCCD camera (Andor iXon +) used to monitor dye optoinjection and perform long-term imaging. All components of the system, such as the SLM, shutter and EMCCD camera, were controlled by a user-friendly software (Labview 8.5) for sequential doses performed in the optoinjection experiments as well as for optical trapping experiments. The multi-modal platform was developed with a "point and shoot" functionality for optoinjection or in the case of optical trapping "point and trap" for ease of use. It was also capable of automated pre-defined displacement of the focal spot allowing a sequenced computer controlled dosage of laser in multiple spatial locations on the blastomere surface, providing enhanced optoinjection efficiency [24].

3. Materials and Methods

3.1 Gametes collection

Adult worms were collected at East Sands, St. Andrews and maintained in natural sea water at ambient temperatures (approximately 15°C during summer). The adult worms (Fig. 1 (B)) were removed from their calcified tubes by breaking open the posterior portion of the tubes and forcing the animals backward. Following de-tubing, fertile animals release their gametes. Male and female worms were transferred separately into Petri dishes. Eggs were rinsed through a 100 μm sieve and then collected into a 40 μm sieve. 1.4 ml of water containing sperm was then added and left for 15 min to allow fertilization to occur. The embryos were washed and then transferred to a dish of fresh sea water. The embryos were kept in a Styrofoam box with an ice pack at one end to maintain the temperature between 14 and 18°C. Two to three hours after fertilization, *P. lamarckii* embryos undergo equal spiral cleavage and subsequent divisions occur variably at 30 min to 1.5 h intervals. Incubating the embryos at cooler temperature slows down their development.

3.2 Sample preparation

P. lamarckii embryos immersed in seawater were placed into 10-mm glass bottom Petri dishes (World Precision Instruments). For optical trapping experiments, the glass-bottom Petri dish was treated by adding 20 mg/ml poly-2-hydroxyethylmethacrylate (Sigma-Aldrich) in 95% ethanol and then allowed to evaporate to prevent the embryos from adhering at the bottom of the dish. Optoinjection experiments were performed with Texas red and Fluorescein fluorescently labeled dextrans with sizes 3 kDa, 10 kDa, 70 kDa and 500 kDa (Invitrogen) and Propidium iodide (PI, Invitrogen) diluted in filtered seawater to a final concentration of 10 μM.

4. Intracellular delivery of macromolecules into living embryos

Ultrastructural studies on eggs of the sister species *Pomatoceros triqueter*, showed that the plasma membrane is first enclosed in a perivitelline space (~500 nm) which is surrounded with a thick chorion (~0.5-1.0 μm). External to this is an intermediate layer (~70-100 nm) and an outer border layer (~70-90 nm) [25]. In the present study, the mechanics of intake of

#141509 - $15.00 USD Received 21 Jan 2011; revised 17 Apr 2011; accepted 13 May 2011; pub. 16 May 2011

fluorescein conjugated dextrans was investigated in early stage embryos by confocal imaging showing negative contrast images of the embryos (Fig. 2).

Staining of the plasma membrane with a lipophilic dye FM4-64 (Invitrogen) of soaked embryos in fluorescein fluorescently labeled dextrans showed that a dextran size of 500 kDa can penetrate through the outer layers but not through the plasma membrane of individual blastomeres of the embryo (data not shown). Embryos were optoinjected at 2-cell (Fig. 2 (A)) and 4-cell (Fig. 2 (B)) stages of development with 3 and 70 kDa fluorescein labeled dextrans. Figure 2(C) and 2(D) show that dextrans can be optoinjected into the blastomeres without the removal of the chorion. Fluorescently labeled dextran of sizes 3, 10, 70 and 500 kDa were found to be successfully optoinjected into individual blastomeres of living embryos. Independent studies showed that dextrans larger than 500 kDa have a very low diffusion ratio in the cytoplasm [26,27]. This implies that dextrans larger than 500 kDa are almost immobile and may not be able to passively diffuse in the cytoplasm of the embryo. Since 70 and 500 kDa correspond to DNA sizes of 106 and 760 bp respectively, they are representative of oligonucleotide sizes that would be desirable to optoinject into these embryos. As a conclusion, individual blastomeres can be targeted without the need to remove the outer membrane of the embryo, leaving it intact during manipulation, which is crucial for proper development and avoids the need to chemically or mechanically remove these layers and membranes.

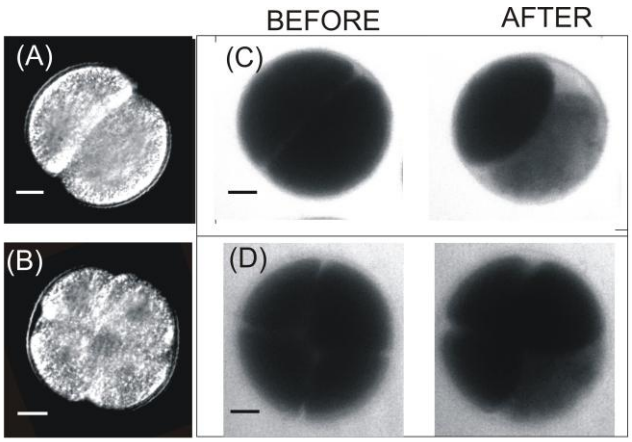

Fig. 2 Images of (A) 2-cell and (B) 4-cell-stage embryos. Images in (C) shows optoinjection of fluorescein labeled dextrans of size 3 kDa to 2-cell and in (D) 70 kDa to 4-cell stage embryo respectively. Bar corresponds to 10 μm.

In the early stages of the embryo (2-cell and 4-cell stages) after optoinjection, the fluorescently labeled dextrans can be seen to perfuse and spread within the individual blastomere within several minutes after the poration event. Similar to previous investigations on cellular poration, the presence of a gas bubble is a good indication of membrane disruption leading to rapid diffusion of the dye into the targeted blastomere [24,28]. However, without the gas bubble, the dye infusion is localized and does not spread throughout the cell. Importantly, cells adjacent to the optoinjected blastomere do not acquire any fluorescence signal, even 30 min after optoinjection, which implies delivery is contained and the dextrans did not pass through any gap junctions at this stage of development.

The poration effects via laser-material interaction are due to the expansion and collapse of short-lived cavitation bubbles produced within a couple of microseconds after irradiation [29]. At sufficiently high laser intensity, long lasting residual gas bubbles lasting from milliseconds to seconds are visible using brightfield imaging [24]. Based on our observations and corroborated by previous independent reports [24,28] the presence of a gas bubble is a good

#141509 - $15.00 USD Received 21 Jan 2011; revised 17 Apr 2011; accepted 13 May 2011; pub. 16 May 2011

indication of successful optoinjection; therefore, we further investigated the parameters required to produce a gas bubble as a function of embryo depth. At 5 μm from the surface of the embryo, only ~0.8 nJ is required to obtain a gas bubble using 30 ms laser exposure. We found that the required pulse energy increases as a function of depth within the embryo, as shown in Fig. 3(A). Probing deeper in the embryo necessitates an increase in the required pulse energy to create gas bubbles which may be due to the combined effects of light scattering within the optically dense sample and increased spherical aberration of the beam with increasing embryo depth. Similar to multiphoton imaging, the combination of increase in spherical aberration and scattering of the beam reduces the multiphoton absorption with increasing depth within the sample [30]. As shown in Fig. 3(A), at a depth of 40 μm into the embryo, the pulse energy required is 2.3 times more compared to 5 μm from the embryo surface.

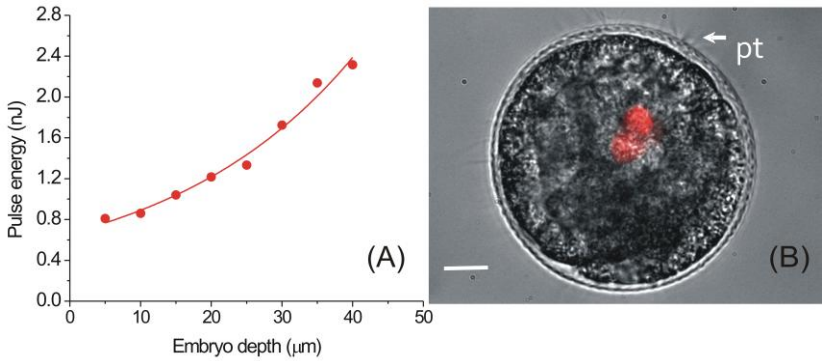

Fig. 3. (A) Pulse energy required to generate a gas bubble as a function of depth of an embryo. (B) An image of a well-developed embryo with 2 optoinjected cells. Pt are prototrochal cilia. Bar corresponds to 10 μm.

To assess the success of optoinjection, *P. lamarckii* embryos of mixed cleavage stages were bathed in a solution of Propidium iodide (PI, Invitrogen) mixed in seawater to a final concentration of ~10 μM. PI was chosen, as it allowed the visualization of fluorescence from blastomeres without the need to wash the embryos. Using this method, we demonstrated the capability of the fs pulse to be focused tightly within the embryo, avoiding collateral damage to the surrounding cells. For example, a larva at the gastrula/early trochophore stage (manifested by the presence of visible prototrochal (pt) cilia) was optoinjected and is shown in Fig. 3(B). Two cells which were 30 μm deep within the embryo were selectively targeted and optoinjected with PI. Notably, cells above the targeted cells were not damaged and did not take up any dye during the process. This 3-D localized optoinjection capability, using fs pulses, could be utilized to follow internal cell lineages in later stage embryos and larvae. This specific delivery of material to internal cells is a unique feature of this optoinjection technique, as delivery by more traditional microinjection would lead to piercing and damaging of cells in the capillary needle injection path.

Table 1. Optoinjection efficiency at varying embryo stage with propidium iodide using the laser power of 65 mW and 30 ms exposure time

Embryo stage	1-cell	1-2 cells	2-16 cells	Late stage
Successfully optoinjected (total number of optoinjected)	10(23)	19(42)	23(43)	26(47)
Percent successful optoinjection	43.5%	45.2%	53.5%	55.3%

Meanwhile, the optoinjection efficiency using PI was determined as a function of cell embryo stage. Each blastomere was targeted at three different locations on its surface forming a sequence of equilateral triangle of targeted dosage points (~1 μm apart) by dynamically

#141509 - $15.00 USD Received 21 Jan 2011; revised 17 Apr 2011; accepted 13 May 2011; pub. 16 May 2011

reconfiguring the phase pattern on the SLM. Individual gas bubbles were present at each of the delivered shot sites on the blastomere surface. Successful optoinjection was visualized 5 min after irradiation by detecting increased in fluorescence at the blastomere optoinjected due to the intake of PI and subsequent intercalation of PI with DNA or mRNA (Table 1). The optoinjection efficiency ranged from nearly 44% for single cell zygotes to 55% for late stage (greater than 16 cells) embryos using laser power of 65 mW and exposure time of 30 ms. For early stage blastomeres, where the surface area is large compared to the later stages, the creation of multiple small to medium sized bubbles on the plasma membrane was required to induce successful optoinjection whilst maintaining the viability of the embryos.

Although the presence of a gas bubble is a precursor to successful optoinjection, we observed that their size and number also correlates with embryo viability and the likelihood of normal development. Subsequent normal cleavage of the optoinjected blastomere was found to be correlated to the size of the bubble, as large bubbles often led to the leakage of blastomere contents, leading to compromised embryo development. Yolk granules and intracellular materials were found to diffuse out of individual blastomeres consistently with large and long lasting gas bubbles. Hence, we next investigated the gas bubble size as a function of varying both laser power (P) and exposure time (T). Each embryo was exposed to the laser only once whilst varying laser power and shutter duration to avoid any cumulative effect during irradiation. The laser was focused on the layer where cortical granules are visible on a single blastomere within the embryo.

The size of gas bubbles was grouped according to varying sizes: small (<1 μm), medium (2-5 μm) and large (>5 μm). These gas bubbles are the result of undissolved biomolecule fragments on the blastomere surface occurring milliseconds to seconds after the formation of low-density plasma [16]. In the literature, the presence of residual gas bubbles is mentioned as an indication of tissue ablation *in vivo* in Drosophila embryos [31]. Visually, the gas bubble size can also indicate successful and viable optoinjection of embryos. Both small and medium

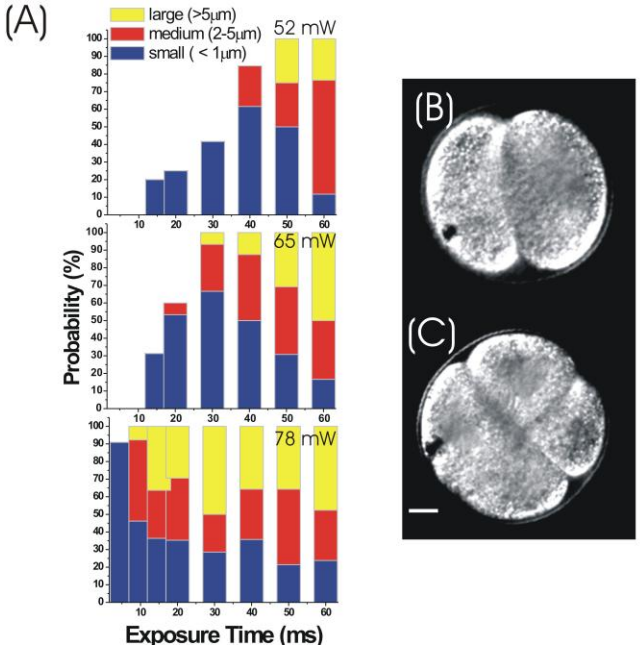

Fig. 4. (A) Gas bubble size as a function of energy dosage. Leakage strongly correlates with the size of the gas bubble. Image in (B) shows a medium size bubble (~4 μm) on a 2- cell stage embryo while (C) shows a large size bubble (~6 μm) in a 4-cell-stage embryo. Embryo in (C) immediately showed leakage of intracellular contents after irradiation. Bar corresponds to 10 μm.

#141509 - $15.00 USD Received 21 Jan 2011; revised 17 Apr 2011; accepted 13 May 2011; pub. 16 May 2011

size gas bubbles led to a high percentage of embryo viability but with varying success of optoinjection. Small size gas bubbles led to only 10-20% successful optoinjection while medium sized gas bubbles resulted in 40-50% successful intake of extracellular material into the blastomeres. Importantly, although the intake is 100% successful with large gas bubbles, it is at the expense of a very low percentage of embryo viability.

The probability of obtaining a specific gas bubble size irrespective of embryo stage is shown in Fig. 4(A). Figure 4(B) and 4(C) shows representative images of medium sized and large sized gas bubble formed at the blastomere surface respectively. It was observed that gas bubbles vary in size as a function of laser power and exposure time. For P = 52 mW at T < 40 ms, the bubbles were predominantly transient and very small (< 1 μm in size). With increasing T, medium sized bubbles with diameters of 2-5 μm were formed. Increasing P to 65 mW, shifted the onset of generating medium to large sized bubbles to a shorter exposure time, from T = 40 ms to T = 20 ms. Medium to large gas bubbles which were more consistently formed at P = 78 mW and with T greater than 10 ms, tended to be long lasting and collapsed only after several seconds.

Of particular importance was the observation that individual blastomeres could carry on dividing following the induction of a gas bubble (Media 1, Fig. 5 (A,B)), as observed by time-lapse recording (Media 2, Fig. 5(C,D)). Time lapse imaging was performed on irradiated embryos over an hour after optoinjection. Two targeted blastomeres in the presence of gas bubbles subsequently divided after irradiation with the fs laser. A percentage of the irradiated embryo carried on dividing and became a normal and viable trochophore larva, 24-48 h post fertilization. We found that 46 ± 8% of the embryos irradiated at 1-4 cell stage developed into proper trochophore larvae compared to 90 ± 3% of the control (non-irradiated) embryos in the absence of dextrans or PI for n = 3 experiments with an average of 50 embryos. Properly developed trochophore larvae were determined by fixing the samples in 4% paraformaldehyde solution and then checking each irradiated larva based on a normal body plan as described in literature [20]. Furthermore, an individual blastomere optoinjected at 2-cell stage with a 3 kDa dextran dye could survive the procedure and carried on dividing into smaller cells which carried the optoinjected dye (see Fig. 5 (E)). A mosaic pattern of tagged cells was typically

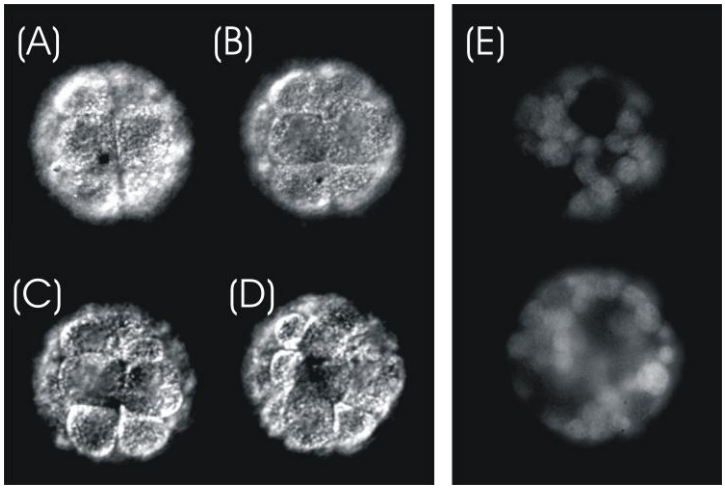

Fig. 5. Image in (A) and (B) shows a bubble created on the blastomeres of an embryo upon irradiation with fs laser (Media 1). Time lapse imaging of the same embryo (Media 2) with still images in (C) showing the blastomeres irradiated have retained morphological features without leakage and in (D) the blastomeres have carried on dividing. (E) Fluorescence images of an embryo at different imaging planes optoinjected with 3 kDa dextran at the early stage that has carried on dividing and shared the dye to its daughter cells.

#141509 - $15.00 USD Received 21 Jan 2011; revised 17 Apr 2011; accepted 13 May 2011; pub. 16 May 2011

observed demonstrating that the optoinjected blastomere remained viable and the injected dye had been passed on to daughter cells. This shows that the proposed technique may be used for cell-lineage mapping both at early and later stages of embryo development.

5. Optical trapping of *P. lamarckii* embryos

The second important functionality of the presented holographic system is the ability to orient, trap and move small embryos. For this experiment the Ti:sapphire laser was switched to CW operation at 800 nm. Clonal growth studies of trapped Chinese hamster ovary cells showed that optical trapping with laser wavelength of 800 nm is significantly less toxic than the conventionally used trapping lasers at around 1064 nm [10]. The SLM-based holographic beam steering was used to translate the focal spot so that individual embryos can be dynamically positioned and oriented in three dimensions.

Single-cell zygotes of *P. lamarckii* were utilized for all optical trapping experiments. Previously, the use of weakly focused beam or a counter-propagating beam configuration has been demonstrated for optical trapping of both particles and cells as opposed to tightly focused beam with NA greater than 1.0. We found that in our system a single beam trap at a laser power of 130 mW weakly focused using a 20×, 0.5 NA objective (Nikon) could levitate the embryos above the glass bottom of the dish and, together with the buoyant force, balance gravity to stably position the embryo at a given height (Fig. 6(A)). At the same time the embryos were confined in the lateral plane resulting in full three dimensional trapping. A gradual change of the phase modulation on the SLM could translate the trap in three dimensions resulting in a controlled movement of the embryo.

Interestingly, in the single beam configuration, the beam induced an optical torque on the embryo causing it to rotate around its axis (Fig. 6(B), Media 3) due to the embryo's inhomogeneity and the mismatch between the position of the beam focus and the centre of mass of the embryo. This may be useful for future studies in which manipulation and long-term imaging studies of embryos requires it to be oriented either at its animal or vegetal pole position. Furthermore, optical orientation allows immediate access and subsequent optoinjection of molecules into specific features in a developed embryo, for example the blastopore lip which forms the mouth and anus.

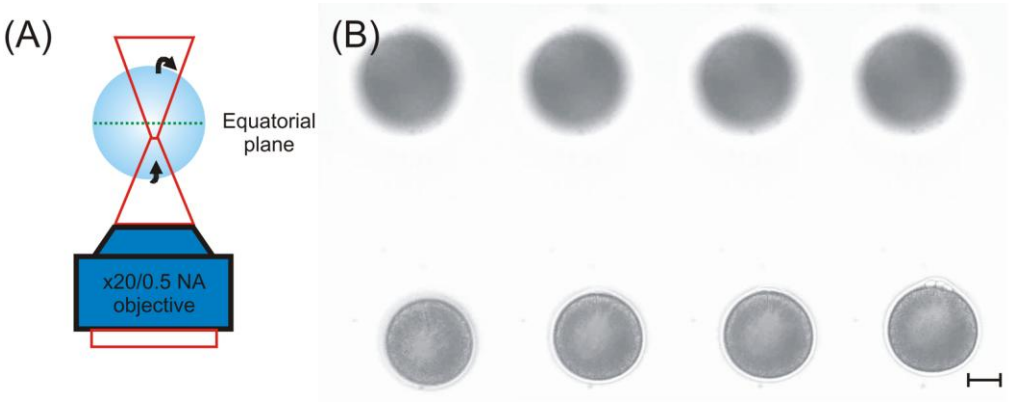

Fig. 6. Single beam optical trap of a *P. lamarckii* embryo. (A) Schematic layout of the optical trap and arrows indicating direction of rotation. (B) Movie stills of optical trapping of embryo using a single beam optical trap (Media 3). Bar corresponds to 20 μm.

In a more advanced approach we used a reconfigurable dual focus trap symmetrically positioned along the z-axis. This allowed stable trapping at a height of up to 200 μm above the glass bottom dish without rotation. Figure 7(A) shows the schematic illustration of the dual focus trap configuration. At 190 μm above the bottom of the dish, the most stable configuration was found when two overlapping foci were axially separated by 36 μm. The

#141509 - $15.00 USD Received 21 Jan 2011; revised 17 Apr 2011; accepted 13 May 2011; pub. 16 May 2011

holographic system enabled dynamic adjustment of the hologram allowing optimization of the locations of the two foci within the embryo and consequently providing the most stable trapping. An example of the phase profile displayed in the SLM for stable optical trapping of the embryo is shown in Fig. 7(B). Using a total laser power of about 175 mW with power equally divided into the two foci, a single embryo can be optically trapped 190 μm above the glass bottom dish as shown in Fig. 7(C). At these parameters, the measured escape speed, defined as the speed at which the embryo drops out of the optical trap is 20 ± 2 μm/s.

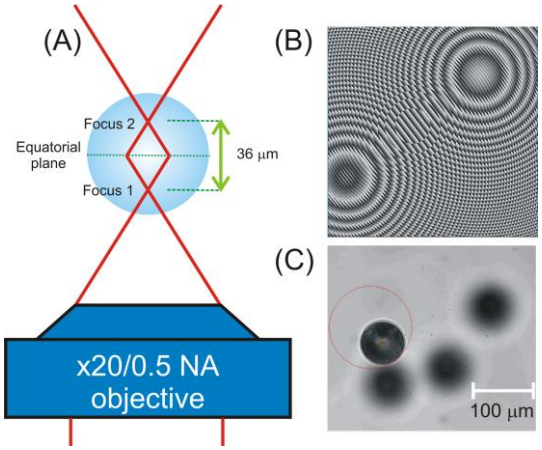

Fig. 7. (A) Schematic illustration of the dual focus trap on a 1-cell *P. lamarckii* embryo. The dual focus trap was created by encoding a phase mask as shown on (B) on the SLM. The two foci were separated 36 μm apart. In this configuration, an embryo can be optically trapped 190 μm above the glass bottom dish. (C) An image of a single embryo stably trapped above the dish and the defocused image of embryos at the bottom of the Petri dish.

An important aspect in this optical approach is maintaining the viability of the embryo trapped. Previous work on optical trapping performed at 1064 nm conducted in water showed that a temperature increase of ~1°C is expected per 100 mW trapping power [11]. As our parameters are within this range and water has substantially lower absorption at 800 nm than at 1064 nm, the local temperature increase should not be detrimental to the optically trapped embryos. Indeed, we verified that optical trapping of single-cell *P. lamarckii* embryos for around 10 min did not induce visible morphological changes and the embryos carried on to subsequent division.water has substantially lower absorption at 800 nm than at 1064 nm, the local temperature increase should not be detrimental to the optically trapped embryos. Indeed, we verified that optical trapping of single-cell *P. lamarckii* embryos for around 10 min did not induce visible morphological changes and the embryos carried on to subsequent division.

6. Conclusions

To conclude, this work demonstrates a system capable of all-optical manipulation of small embryos. The proposed holographic optoinjection and trapping system facilitates a computer-controlled optical handling and time-sequenced laser dosage of embryos paving the way towards automated high-throughput processing. The system allows selective optoinjection of small molecules into cells deep within a *P. lamarckii* embryo. Size of the gas bubbles formed was found to correlate inversely with subsequent correct development of the embryos. Time lapse imaging confirmed that the presence of less than 5 μm sized gas bubbles is not detrimental to the irradiated blastomere. Potential applications for this technology would include cell lineage mapping and genetic modification to form transgenic animals. Furthermore, the same system can be utilized for optical trapping, moving and orientation of these embryos. We believe that the field of developmental biology may greatly benefit from

#141509 - $15.00 USD Received 21 Jan 2011; revised 17 Apr 2011; accepted 13 May 2011; pub. 16 May 2011

the development of robust all-optical techniques for injection, gene transfection and manipulation of embryos, such as these presented above.

Acknowledgments

The authors would like to thank Scottish Universities Life Sciences Alliance (SULSA) and the Engineering Physical Sciences Research Council (EPSRC) for funding. MLTM acknowledges the support of a SUPA Prize Studentship. DEKF acknowledges the support of the Royal Society. KD is a Royal Society Wolfson Merit Award holder.

#141509 - $15.00 USD Received 21 Jan 2011; revised 17 Apr 2011; accepted 13 May 2011; pub. 16 May 2011